Novel method for searching for the $\Xi_c^{0/+}$-$\Xi_c^{\prime 0/+}$ mixing effect in the angular distribution analysis of a four-body $\Xi_c^{0/+}$ decay

Zhi-Peng Xing[1,*] and Yu-Ji Shi[2,†]

[1]Tsung-Dao Lee Institute, Shanghai Jiao Tong University, Shanghai 200240, People's Republic of China
[2]School of Physics, East China University of Science and Technology, Shanghai 200237, China

(Received 20 January 2023; accepted 20 March 2023; published 19 April 2023)

In this work, we raise a novel method for searching for the Ξ_c^{0+}-$\Xi_c^{0+\prime}$ mixing effect in an angular distribution analysis of the $\Xi_c \to \Xi^{(\prime)}(\Lambda\pi)\ell^+\nu$ decay, where the mixing effect can be observed by the appearance of the Ξ' resonance. Armed with this angular distribution, the branching fraction and the forward-backward asymmetry are predicted. We point out that the forward-backward asymmetry, as a function of the invariant mass square of $\Xi^{(\prime)}$ and the Ξ_c^{0+}-$\Xi_c^{0+\prime}$ mixing angle θ_c, can be used to distinguish the two resonances $\Xi^{(\prime)}$ and even provide a possibility to determine the exact mixing angle.

DOI: 10.1103/PhysRevD.107.074024

I. INTRODUCTION

Particle physics describes all the fundamental materials and interactions in our universe. After 2012, all the elementary particles predicted by the Standard Model (SM) had been observed [1,2], which makes the SM a widely accepted theory for particle physics. However, it has been widely recognized that the SM is just an effective theory of a much more fundamental one, where the relevant energy scale far exceeds the detection capabilities of current experiments. The physics beyond the SM or the so-called New Physics (NP), if discovered by these experiments, will provide critical clues for us to construct the fundamental theory. In the past decade, some signs of NP have been observed by various experimental groups [3–6].

Heavy flavor physics offers one of the ideal platforms for searching for NP. Recently, some anomalies in heavy meson decays such as $R_{K^{(*)}}$ [7] and $R_{D^{(*)}}$ [8,9] have been observed, which implies the existence of NP. Besides the heavy mesons, nowadays the heavy baryon or especially the charm baryon decays have attracted the attention of the experiments [10], and a number of charm baryon decay channels have been measured by many experimental collaborations, such as Belle [11,12], LHCb [13], and BESIII [14,15].

In the last two years, the puzzle about the branching fraction of the $\Xi_c^{0/+} \to \Xi^{-/0}\ell^+\nu$ decays has emerged from the deviation between the experimental measurements and theoretical predictions [16–18]. In our previous research [19], the branching fraction $\mathcal{B}(\Xi_c^0 \to \Xi^- e^+\nu)$ from the SU(3) symmetry prediction had six σ standard deviation from the experimental data [20,21]. Furthermore, not only the semi- but also the nonleptonic charm baryon decays have the SU(3) symmetry breaking effect [22]. On the theoretical side, the $\Xi_c^{0/+}$-$\Xi_c^{\prime 0/+}$ mixing effect is the most possible reason for explaining this puzzle [19,23–26]. However, on the experimental side, it is difficult to search for such mixing directly since it always emerges in the complex baryonic transitions. Therefore, finding a suitable method to search for the $\Xi_c^{0/+}$-$\Xi_c^{\prime 0/+}$ mixing effect is the main task of this work.

In this work, we choose the four-body decay $\Xi_c \to \Xi^{(\prime)}(\Lambda\pi)\ell^+\nu$ as an ideal channel to search for the $\Xi_c^{0/+}$-$\Xi_c^{\prime 0/+}$ mixing. Here Ξ is a spin-1/2 octet state and Ξ' is a spin-3/2 decuplet state. In principle, this mixing enables Ξ_c^{0+} to decay into Ξ', so one should observe both the two resonances Ξ and Ξ' in this decay channel. However, the $\Xi_c \to \Xi'(\Lambda\pi)\ell^+\nu$ is highly suppressed due to two reasons. The first reason is that the $\Xi_c \to \Xi'$ process is suppressed by $\sin\theta_c$ with θ_c being the mixing angle. The second reason is that the strong decay width of $\Xi' \to \Lambda\pi$ is much smaller than that of $\Xi \to \Lambda\pi$. Therefore this channel can hardly be observed by the experiments. Instead of the branching fraction, we propose the angular distributions of $\Xi_c \to \Xi^{(\prime)}(\Lambda\pi)\ell^+\nu$ to search for the $\Xi_c^{0/+}$-$\Xi_c^{\prime 0/+}$ mixing. Note that Ξ and Ξ' have different spins, which will lead to different angular distributions of the $\Lambda\pi$ states. It is possible for the experiments to distinguish the two resonances Ξ and Ξ' by distinguishing two exactly different angular distributions.

*zpxing@sjtu.edu.cn
†Corresponding author.
shiyuji@ecust.edu.cn

This paper is organized as follows. In Sec. II, we give the theoretical framework of this work, where the helicity amplitudes for $\Xi_c \to \Xi^{(\prime)}(\Lambda\pi)\ell^+\nu$ decays are adopted to derive the angular distributions. In Sec. III, we give the angular distributions analysis of this process and put forward an observable for searching for the $\Xi_c^{0/+}$-$\Xi_c^{\prime 0/+}$ mixing effect. In Sec. IV, the numerical results are performed using the form factors from Lattice calculation, light cone sum rules, and the light-front quark model in order to validate our analysis. In the last section, a brief summary will be presented. Some calculation details are collected in the Appendix.

II. HELICITY AMPLITUDE

The deviation between theoretical prediction and experimental results can be explained by the $\Xi_c^{0/+}$-$\Xi_c^{\prime 0/+}$ mixing [19,24]. The $\Xi_c^{0/+}$-$\Xi_c^{\prime 0/+}$ mixing is a very natural assumption since the quantum number such as spin and parity is same $\frac{1}{2}^+$ for both $\Xi_c^{0/+}$ and $\Xi_c^{\prime 0/+}$. In previous studies [19], the mixing effect was introduced quite naturally by considering the mass division of the strange quark and up/down quarks.

After the mixing the physical state ($\Xi_c^{0/+p}$) is expressed as

$$\Xi_c^{0/+p} = \Xi_c^{0/+}\cos\theta_c + \Xi_c^{\prime 0/+}\sin\theta_c, \tag{1}$$

where $\Xi_c^{(\prime)0+}$ are the flavor eigenstates. The physical state Ξ_c^p can decay into a decuplet baryon state Ξ' which is forbidden without the mixing effect. Therefore the processes $\Xi_c^p \to \Xi'\ell^+\nu$ can be used to search for the mixing effect. However, as mentioned before it is difficult to measure this process directly because the $\Xi_c^p \to \Xi'\ell^+\nu$ will be suppressed by the factor $\sin\theta_c$.

To search for the forbidden process $\Xi_c^p \to \Xi'\ell^+\nu$, we will focus on the cascade decay process $\Xi_c^p \to \Xi^{(\prime)}(\Lambda\pi)\ell^+\nu$. Although the resonance Ξ' may have a tiny contribution which can be seen as the systemic error, the angular distribution will provide additional information about the decay processes.

The kinematics of Ξ_c^p cascade decay are shown in Fig. 1. In the rest frame of the initial state Ξ_c^p, the $\Xi^{(\prime)}$ moves along the z-axis. The angle ϕ is defined as the angle between the leptonic decay plane and $\Xi^{(\prime)}$ cascade decay plane, while $\theta(\theta_\Lambda)$ is the angle between the moving direction of $\ell^+(\Lambda)$ and the positive (negative) direction of the z-axis.

Using the Breit-Wigner form for the resonance, we can divide the amplitude of the cascade decay into several Lorentz-invariant parts such as

$$\begin{aligned}&\mathcal{M}(\Xi_c^p \to \Xi^{(\prime)}(\Lambda\pi)\ell^+\nu)\\ &= \sum_{J_{\Xi^{(\prime)}}}\sum_{s_{\Xi^{(\prime)}}} i\mathcal{M}(\Xi_c^p \to \Xi^{(\prime)}\ell^+\nu)\\ &\quad\times\frac{i}{p_\Xi^2 - m_{\Xi^{(\prime)}}^2 + im_{\Xi^{(\prime)}}\Gamma_{\Xi^{(\prime)}}} i\mathcal{M}(\Xi^{(\prime)} \to \Lambda\pi),\end{aligned} \tag{2}$$

with the momentum of resonance $p_\Xi^\mu = p_\Lambda^\mu + p_\pi^\mu$.

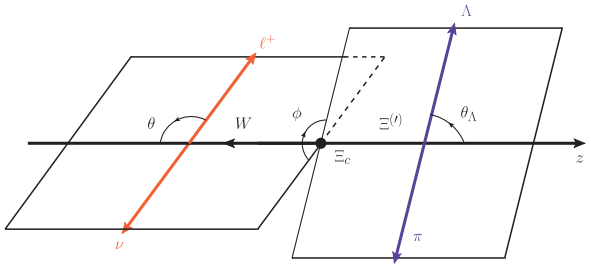

FIG. 1. The kinematics for the $\Xi_c^p \to \Xi^{(\prime)}(\Lambda\pi)\ell^+\nu$. In the Ξ_c^p baryon rest frame, the $\Xi^{(\prime)}$ moves along the z-axis. The $\theta(\theta_\Lambda)$ is defined as the angle between negative (positive) z-axis and the moving direction of ℓ^+ (Λ) in the W ($\Xi^{(\prime)}$) rest frame. The ϕ is the angle between the $\Xi^{(\prime)}$ and W cascade decay planes.

For the $\Xi_c^p \to \Xi^{(\prime)}\ell^+\nu$ process, the relevant effective Hamiltonian is

$$\mathcal{H}_{c\to s} = \frac{G_F}{\sqrt{2}}[V_{cs}^*\bar{s}\gamma^\mu(1-\gamma_5)c\bar{\nu}\gamma_\mu(1-\gamma_5)\ell] + \text{H.c.}. \tag{3}$$

With the use of this effective Hamiltonian, the decay amplitude is written as the production of hadronic helicity amplitude and leptonic helicity amplitude:

$$\begin{aligned}i\mathcal{M}(\Xi_c^p \to \Xi^{(\prime)}\ell^+\nu) &= \sum_{s_w}\frac{G_F}{\sqrt{2}}V_{cs}^*\bar{u}_\nu\gamma_\rho(1-\gamma_5)\nu_\ell\epsilon^\rho(s_w)\\ &\quad\times\langle\Xi^{(\prime)}|\bar{s}\gamma^\mu(1-\gamma_5)c|\Xi_c^p\rangle\epsilon_\mu^*(s_w)\\ &= \sum_{s_w}\frac{G_F}{\sqrt{2}}V_{cs}^*L_{s_\ell}^{s_w}(\phi,\theta)\times h_{s_w,s_\Xi^{(\prime)}}^{s_{\Xi_c}}.\end{aligned} \tag{4}$$

The Lorentz-invariant amplitude $i\mathcal{M}(\Xi^{(\prime)} \to \Lambda\pi)$ can be described by the Wigner function and is parametrized as [27]

$$i\mathcal{M}(\Xi^{(\prime)} \to \Lambda\pi) = \mathcal{A}^{(\prime)} \times D_{s_{\Xi^{(\prime)}},s_\Lambda}^{J_\Xi}(\phi_\Xi,\theta_\Lambda), \tag{5}$$

where J_Ξ is the total spin of $\Xi^{(\prime)}$ and $s_{\Xi^{(\prime)}}$, and s_Λ are the helicities of $\Xi^{(\prime)}$ and Λ respectively. The $D_{s_{\Xi^{(\prime)}},s_\Lambda}^{J_\Xi}(\phi_\Xi,\theta_\Lambda)$ is the Wigner function [28] and ϕ_Ξ is the angle of the $\Xi^{(\prime)}\Lambda\pi$ plane and x-z plane. The ϕ_Ξ is setting as 0 because there are three degrees of freedom in angle in the cascade decay process, and the x-z plane and $\Xi^{(\prime)}\Lambda\pi$ plane can coincide in our work. The coefficient $\mathcal{A}^{(\prime)}$ can be determined by the decay width $\Gamma(\Xi^{(\prime)} \to \Lambda\pi)$:

$$\begin{aligned}A &= \sqrt{\Gamma(\Xi \to \Lambda\pi)8\pi m_\Xi^2/|p_\Lambda|}\\ A' &= \sqrt{\Gamma(\Xi' \to \Lambda\pi)16\pi m_{\Xi^{(\prime)}}^2/|p_\Lambda|}.\end{aligned} \tag{6}$$

Then the total amplitude is expressed as

$$\begin{aligned}\mathcal{M}(\Xi_c^p \to \Xi^{(\prime)}(\Lambda\pi)\ell^+\nu) &= \sum_{J_{\Xi^{(\prime)}}} \sum_{s_{\Xi^{(\prime)}},s_w} \frac{G_F}{\sqrt{2}} V_{cs}^* \\ &\times H^{J_{\Xi^{(\prime)}}}_{s_{\Xi_c},s_{\Xi^{(\prime)}}} L^{s_w}_{s_\ell}(\phi,\theta) D^{J_\Xi}_{s_{\Xi^{(\prime)}},s_\Lambda}(\phi_\Xi,\theta_\Lambda), \\ H^{J_{\Xi^{(\prime)}}}_{s_{\Xi_c},s_{\Xi^{(\prime)}}} &= \frac{iA^{(\prime)}}{p^2_{\Xi^{(\prime)}} - m^2_{\Xi^{(\prime)}} + im_{\Xi^{(\prime)}}\Gamma_{\Xi^{(\prime)}}} h^{s_{\Xi_c}}_{s_w,s^{(\prime)}_\Xi} \\ &= L_{\Xi^{(\prime)}} h^{s_{\Xi_c}}_{s_w,s^{(\prime)}_\Xi}. \end{aligned} \tag{7}$$

The differential decay width is expressed as [29]:

$$d\Gamma = d\Pi_4 \times \frac{(2\pi)^4}{2m_{\Xi_c}} |\mathcal{M}(\Xi_c^p \to \Xi^{(\prime)}(\Lambda\pi)\ell^+\nu)|^2, \tag{8}$$

where $d\Pi_4$ is four-body phase space integration.

III. ANGULAR DISTRIBUTION

The differential decay width and other relevant observables of the four-body decay $\Xi_c \to \Xi^{(\prime)}(\Lambda\pi)\ell^+\nu$ depend on the angle $\phi, \theta, \theta_\Lambda$ as shown in Fig. 1. Now, expanding the Wigner function and the leptonic helicity amplitudes in the differential decay width, we arrive at the deferential decay width in the Appendix. The resonance Ξ' can be detected by analyzing the shape of the differential decay width $d\Gamma/dp^2_\Xi$ as a function of p^2_Ξ, which reads as

$$\frac{d\Gamma}{dp^2_\Xi} = \frac{8\pi}{9}\mathcal{P}(9L_{11} - 3L_{13} - 3L_{41} + L_{44}), \tag{9}$$

where the function L_{ij} are shown in the Appendix. This observable will have a peak around the $p^2_\Xi = m^2_{\Xi'}$ according to the Breit-Wigner form of the resonance. The contribution from each resonance is proportional to the branching fraction $\mathcal{B}(\Xi^{(\prime)} \to \Lambda\pi)$. Therefore the process $\Xi_c^p \to \Xi'\ell^+\nu$ is very difficult to observe since the branching fraction $\mathcal{B}(\Xi' \to \Lambda\pi)$ is extremely small.

Besides the decay width the forward-backward asymmetry is another important observable. In this work, we define the normalized forward-backward asymmetry $A_{\rm FB}$ as

$$\begin{aligned}\frac{dA_{\rm FB}}{dp^2_\Xi} &= \frac{[\int_0^1 - \int_{-1}^0] d\cos\theta_\Lambda \frac{d\Gamma}{dp^2_\Xi d\cos\theta_\Lambda}}{\int_{-1}^1 d\cos\theta_\Lambda \frac{d\Gamma}{dp^2_\Xi d\cos\theta_\Lambda}} \\ &= \frac{3}{2}\frac{3L_{12} - L_{33}}{9L_{11} - 3L_{13} - 3L_{41} + L_{44}} \\ &= \frac{4}{3}\frac{\sum_{s_{\Xi_c},s_\Xi} \mathcal{R}_e(H^{\frac{1}{2}}_{s_{\Xi_c},s_\Xi} H^{\frac{3}{2}*}_{s_{\Xi_c},s_\Xi})}{\sum_{s_{\Xi_c},s_{\Xi^{(\prime)}}} (2|H^{\frac{1}{2}}_{s_{\Xi_c},s_\Xi}|^2 + |H^{\frac{3}{2}}_{s_{\Xi_c},s_{\Xi'}}|^2)}, \end{aligned} \tag{10}$$

where

$$\begin{aligned}&\sum_{s_{\Xi_c},s_\Xi} \mathcal{R}_e\left(H^{\frac{1}{2}}_{s_{\Xi_c},s_\Xi} H^{\frac{3}{2}*}_{s_{\Xi_c},s_\Xi}\right) \\ &= \frac{(p^2_\Xi - m^2_\Xi)(p^2_\Xi - m_{\Xi'}) - \Gamma_\Xi m_\Xi \Gamma_{\Xi'} m_{\Xi'}}{((p^2_\Xi - m^2_\Xi)^2 + \Gamma^2_\Xi m^2_\Xi)((p^2_\Xi - m^2_{\Xi'})^2 + \Gamma^2_{\Xi'} m^2_{\Xi'})} \\ &\times (\cos\theta_c h^{3,s_{\Xi_c}}_{s_w,s_\Xi} + \sin\theta_c h^{6,s_{\Xi_c}}_{s_w,s_\Xi}) \sin\theta_c h^{6,s_{\Xi_c}}_{s_w,s'_\Xi}. \end{aligned} \tag{11}$$

$h^{3,s_{\Xi_c}}_{s_w,s_\Xi}$ and $h^{6,s_{\Xi_c}}_{s_w,s^{(\prime)}_\Xi}$ is the hadronic matrix element with the triplet charm baryon and sextet charm baryon as

$$\begin{aligned} h^{3,s_{\Xi_c}}_{s_w,s_\Xi} &= \langle \Xi|\bar{s}\gamma^\mu(1-\gamma_5)c|\Xi_c\rangle \epsilon^*_\mu(s_w), \\ h^{6,s_{\Xi_c}}_{s_w,s^{(\prime)}_\Xi} &= \langle \Xi^{(\prime)}|\bar{s}\gamma^\mu(1-\gamma_5)c|\Xi'_c\rangle \epsilon^*_\mu(s_w). \end{aligned} \tag{12}$$

It can be found that the forward-backward asymmetry is proportional to the interference of the amplitudes induced by the Ξ and Ξ' resonances. Therefore, although the amplitudes induced by Ξ' are suppressed due to the tiny decay width of $\Xi' \to \Lambda\pi$, $A_{\rm FB}$ is still enhanced by the amplitudes induced by Ξ, which makes it possible to measure $A_{\rm FB}$ by the experiments. Furthermore, since the $A_{\rm FB}$ obtained here is a function of θ_c, we can determine this mixing angle as soon as the exact value of $A_{\rm FB}$ is measured. We will give the θ_c dependence of $A_{\rm FB}$ in Sec. III.

On the other hand, as we discussed in Ref. [27], it is possible to distinguish the resonances with different spins by $A_{\rm FB}$. For the decay process of this work, the $dA_{\rm FB}/dp^2_\Xi$ will have two zero points, $s_1 \sim m^2_\Xi$, $s_2 \sim m^2_{\Xi'}$, which can be obtained by solving the equation:

$$\begin{aligned}&\sum_{s_{\Xi_c},s_\Xi} \mathcal{R}_e\left(H^{\frac{1}{2}}_{s_{\Xi_c},s_\Xi} H^{\frac{3}{2}*}_{s_{\Xi_c},s_\Xi}\right) \\ &\propto \frac{(p^2_\Xi - m^2_\Xi)(p^2_\Xi - m_{\Xi'}) - \Gamma_\Xi m_\Xi \Gamma_{\Xi'} m_{\Xi'}}{((p^2_\Xi - m^2_\Xi)^2 + \Gamma^2_\Xi m^2_\Xi)((p^2_\Xi - m^2_{\Xi'})^2 + \Gamma^2_{\Xi'} m^2_{\Xi'})} \\ &= 0. \end{aligned} \tag{13}$$

The solutions read as

$$\begin{aligned} s_1 &= \frac{1}{2}\left(m^2_\Xi + m^2_{\Xi'} - \sqrt{(m^2_\Xi - m^2_{\Xi'})^2 - 4\Gamma_\Xi m_\Xi \Gamma_{\Xi'} m_{\Xi'}}\right) \\ &= m^2_\Xi - \frac{\Gamma_\Xi m_\Xi \Gamma_{\Xi'} m_{\Xi'}}{m^2_{\Xi'} - m^2_\Xi} + O(\Gamma_{\Xi'})^2, \\ s_2 &= \frac{1}{2}\left(m^2_\Xi + m^2_{\Xi'} + \sqrt{(m^2_\Xi - m^2_{\Xi'})^2 - 4\Gamma_\Xi m_\Xi \Gamma_{\Xi'} m_{\Xi'}}\right) \\ &= m^2_{\Xi'} + \frac{\Gamma_\Xi m_\Xi \Gamma_{\Xi'} m_{\Xi'}}{m^2_{\Xi'} - m^2_\Xi} + O(\Gamma_{\Xi'})^2. \end{aligned} \tag{14}$$

Note that $\Gamma_{\Xi'(1530)} = 0.0091$ GeV is extremely small, thus only using the leading term of each solution is precise enough for the following studies. Now, $dA_{\rm FB}/dp_\Xi^2$ has two zero points and each one is around the mass pole of Ξ or Ξ'. This enables us to distinguish the two resonances and provides the evidence of the $\Xi_c^{0/+}$-$\Xi_c^{0/+\prime}$ mixing.

IV. NUMERICAL ESTIMATION

In this section, we will give a numerical estimation by calculating the hadronic matrix element $h^{s_{\Xi_c}}_{s_w,s_\Xi^{(\prime)}}$ with the form factors from Lattice results [17], light cone sum rules [30], and the light-front quark model [31]. The hadronic matrix element is defined as

$$h^{s_{\Xi_c}}_{s_w,s_\Xi^{(\prime)}} = \langle \Xi^{(\prime)}|\bar{s}\gamma^\mu(1-\gamma_5)c|\Xi_c^p\rangle\epsilon_\mu^*(s_w), \tag{15}$$

where the initial state $|\Xi_c^p\rangle$ is physical state, which is the mixing state of the triplet and sextet charm baryon state in Eq. (1). Then the matrix element can be expressed as

$$\begin{aligned}\langle \Xi|\bar{s}\gamma^\mu(1-\gamma_5)c|\Xi_c^p\rangle &= \cos\theta_c\langle \Xi|\bar{s}\gamma^\mu(1-\gamma_5)c|\Xi_c\rangle \\ &\quad + \sin\theta_c\langle \Xi|\bar{s}\gamma^\mu(1-\gamma_5)c|\Xi_c'\rangle \\ \langle \Xi'|\bar{s}\gamma^\mu(1-\gamma_5)c|\Xi_c^p\rangle &= \sin\theta_c\langle \Xi'|\bar{s}\gamma^\mu(1-\gamma_5)c|\Xi_c'\rangle. \end{aligned}\tag{16}$$

These hadronic matrix elements can be expressed by form factors such as

$$\begin{aligned}\langle \Xi|\bar{s}\gamma^\mu(1-\gamma_5)c|\Xi_c\rangle &= \times\Big(\bar{u}(p_\Xi,s_\Xi)\Big[f_1\gamma^\mu + \frac{i\sigma^{\mu\nu}q_\nu}{m_{\Xi_c}}f_2 + \frac{q^\mu}{m_{\Xi_c}}f_3\Big]u(p_{\Xi_c},s_{\Xi_c}) \\ &\quad - \bar{u}(p_\Xi,s_\Xi)\Big[g_1\gamma^\mu + \frac{i\sigma^{\mu\nu}q_\nu}{m_{\Xi_c}}g_2 + \frac{q^\mu}{m_{\Xi_c}}g_3\Big]\gamma_5 u(p_{\Xi_c},s_{\Xi_c})\Big), \\ \langle \Xi|\bar{s}\gamma^\mu(1-\gamma_5)c|\Xi_c'\rangle &= \times\Big(\bar{u}(p_\Xi,s_\Xi)\Big[f_1'\gamma^\mu + \frac{i\sigma^{\mu\nu}q_\nu}{m_{\Xi_c}}f_2' + \frac{q^\mu}{m_{\Xi_c}}f_3'\Big]u(p_{\Xi_c},s_{\Xi_c}) \\ &\quad - \bar{u}(p_\Xi,s_\Xi)\Big[g_1'\gamma^\mu + \frac{i\sigma^{\mu\nu}q_\nu}{m_{\Xi_c}}g_2' + \frac{q^\mu}{m_{\Xi_c}}g_3'\Big]\gamma_5 u(p_{\Xi_c},s_{\Xi_c})\Big), \\ \langle \Xi'|\bar{s}\gamma^\mu(1-\gamma_5)c|\Xi_c'\rangle &= \Big(\bar{u}_\rho(p_\Xi,s_{\Xi'})\Big[\Big(F_1\gamma^\mu + \frac{p_{\Xi_c}^\mu}{m_{\Xi_c}}F_2 + \frac{p_{\Xi'}^\mu}{m_{\Xi'}}F_3\Big)\frac{p_{\Xi_c}^\rho}{m_{\Xi_c}} + g^{\mu\rho}F_4\Big]\gamma_5 u(p_{\Xi_c},s_{\Xi_c}) \\ &\quad - \bar{u}_\rho(p_\Xi,s_{\Xi'})\Big[\Big(G_1\gamma^\mu + \frac{p_{\Xi_c}^\mu}{m_{\Xi_c}}G_2 + \frac{p_{\Xi'}^\mu}{m_{\Xi'}}G_3\Big)\frac{p_{\Xi_c}^\rho}{m_{\Xi_c}} + g^{\mu\rho}G_4\Big]u(p_{\Xi_c},s_{\Xi_c})\Big). \end{aligned}\tag{17}$$

The form factors of $\Xi_c \to \Xi$ are evaluated in Lattice QCD [29]. The form factors of $\Xi_c' \to \Xi$ are evaluated by light cone sum rules in Ref. [30]. The form factors of $\Xi_c' \to \Xi'$ are derived by the SU(3) relations [32] with form factors of $\Omega_c \to \Omega$ process which is evaluated in Ref. [31] with the light-front quark model. Note that although this literature only calculated the form factors for $\Omega_c \to \Omega$, using SU(3) relations we can transform them into those for $\Xi_c' \to \Xi'$ by simply multiplying a factor $\sqrt{2/3}$ on them.

In our analysis, we do not distinguish the processes $\Xi_c^{p0} \to \Xi^{(\prime)-}(\Lambda\pi)e^+\nu$ and $\Xi_c^{p+} \to \Xi^{(\prime)0}(\Lambda\pi)e^+\nu$. Therefore, it is suitable to give the numerical analysis for the $\Xi_c^{p0} \to \Xi^{(\prime)-}(\Lambda\pi)e^+\nu$ process as an example. In the first step, the $\mathcal{B}(\Xi_c^p \to \Xi^{(\prime)}e^+\nu_e)$ can be estimated as it does not require the information of $\mathcal{B}(\Xi_c^{(\prime)} \to \Lambda\pi)$ and the mixing angle can be evaluated as $\theta_c = -0.164\pi$ compared to the Belle data $\mathcal{B}(\Xi_c^p \to \Xi e^+\nu_e) = (1.31 \pm 0.04 \pm 0.03 \pm 0.38)\%$ [20].

We also noted that the mixing angle is evaluated as $\theta_c = \pm 0.137\pi$ in Ref. [24]. The $\mathcal{B}(\Xi_c^p \to \Xi^{(\prime)}e^+\nu_e)$ with $\theta_c = \pm 0.137\pi$ are given as

$$\begin{aligned}&\mathcal{B}(\Xi_c^p \to \Xi' e^+\nu_e) = 3.5\times 10^{-4}, \\ &\mathcal{B}(\Xi_c^p \to \Xi e^+\nu_e) = 12.3\%, \qquad \theta_c = 0.137\pi, \\ &\mathcal{B}(\Xi_c^p \to \Xi' e^+\nu_e) = 3.5\times 10^{-4}, \\ &\mathcal{B}(\Xi_c^p \to \Xi e^+\nu_e) = 0.5\%, \qquad \theta_c = -0.137\pi. \end{aligned}\tag{18}$$

In our calculation, the branching fraction $\mathcal{B}(\Xi' \to \Lambda\pi)$ is determined by SU(3) flavor symmetry prediction $\mathcal{B}(\Xi' \to \Lambda\pi) = 5.02\times 10^{-13}$ [33] since it has not been detected in experiments yet. For the decay width, the numerical results can be derived by integrating out the p_Ξ^2, q^2 and angle $\theta, \phi, \theta_\Lambda$ with the $\theta_c = -0.164\pi$ and $\theta_c = \pm 0.137\pi$ in Table I.

TABLE I. Numerical results of the decay width, branching ratio, and forward-backward asymmetry, where the Ξ^- or Ξ'^- in $\Gamma(\Xi'^-)$ and $\mathcal{B}(\Xi^{(\prime)-})$ represent the possible resonance in the cascade decay process $\Xi_c^0 \to \Xi^{(\prime)-}(\Lambda\pi)e^+\nu$.

Observables	$\theta_c = 0.137\pi$	$\theta_c = -0.137\pi$	$\theta_c = -0.164\pi$
$\Gamma(\Xi^-)$ (GeV)	2.476×10^{-13}	2.198×10^{-14}	1.678×10^{-14}
$\Gamma(\Xi'^-)$ (GeV)	4.975×10^{-28}	4.975×10^{-28}	4.975×10^{-28}
$\Gamma(\Xi^{(\prime)-})$ (GeV)	2.476×10^{-13}	2.198×10^{-14}	1.678×10^{-14}
$\mathcal{B}(\Xi^{(\prime)-})(\%)$	5.68	0.504	0.385
$A_{\rm FB}(\mathrm{GeV}^2)$	0.0647	−0.0557	−0.0466

When the mixing angle θ_c becomes zero, the branching fraction of the process will become $\mathcal{B}(\Xi_c^{p0} \to \Xi^-(\Lambda\pi)e^+\nu) = 2.4\%$. It is consistent with the previous work [29]. We also present the differential decay width $d\Gamma/dp_\Xi^2$ as a function of p_Ξ^2 with different θ_c in Fig. 2. In this figure, one can find that the contribution of the Ξ' resonances is tiny. Since the initial state Ξ_c^p is the mixing state of the triplet and sextet charmed baryon, our result will also depend on the mixing angle. Therefore we also present the θ_c dependence in Fig. 2.

For the forward-backward asymmetry, we can estimate its value by integrating out the p_Ξ^2 in Eq. (10) and obtain its value with different θ_c in Table I. Since $A_{\rm FB}$ is sensitive to the mixing angle θ_c, we can study the θ_c dependence of $A_{\rm FB}$. The distribution of $A_{\rm FB}(\theta_c)$ is shown in Fig. 3. One can easily find that $A_{\rm FB}$ is zero when the mixing angle vanishes $\theta_c = 0$ and increases with the growing of θ_c in $\theta_c > 0$ region. However, $A_{\rm FB}$ gives a very interesting curve in the $\theta_c < 0$ region. For the $\theta_c > 0$ case, $A_{\rm FB}$ is determined by the offset between values in the $p_\Xi^2 \in [m_\Xi^2, m_{\Xi'}^2]$ and $p_\Xi^2 > m_{\Xi'}^2$ regions. But for the $\theta_c < 0$ case, since the $\sin(\theta_c)$ is negative, there is a third zero point s_3 appearing in the figure (c, d) of Fig. 3. This zero point can be determined by the equation as

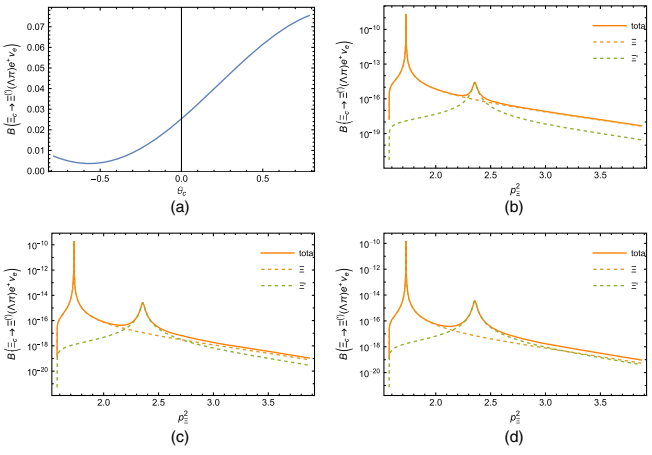

FIG. 2. Branching fraction as functions of the mixing angle (a) and p_Ξ^2 with $\theta_c = 0.137\pi$ (b), $\theta_c = -0.137\pi$ (c), and $\theta_c = -0.164\pi$ (d).

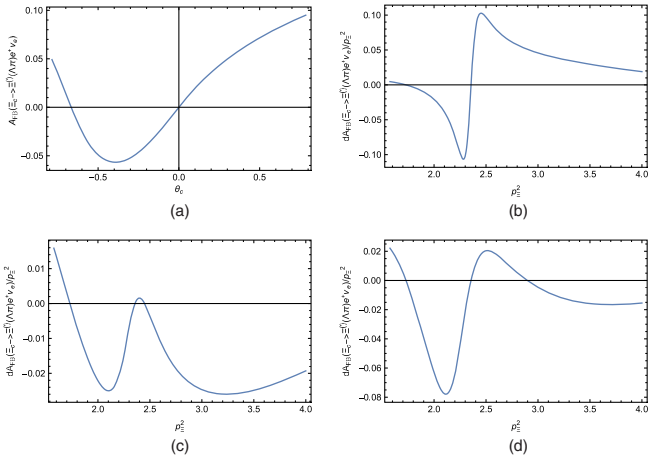

FIG. 3. Forward-backward asymmetry as functions of the mixing angle (a) and p_Ξ^2 with $\theta_c = 0.137\pi$ (a), $\theta_c = -0.137\pi$ (b), and $\theta_c = 0.164\pi$ (c).

$$\cos\theta_c h_{s_w,s_\Xi}^{3,s_{\Xi_c}} + \sin\theta_c h_{s_w,s_\Xi}^{6,s_{\Xi_c}} = 0. \tag{19}$$

When $p_\Xi^2 > s_3$, the value of $A_{\rm FB}$ is negative and therefore the total value of $A_{\rm FB}$ is negative. This analysis can be confirmed in p_Ξ^2 dependence $A_{\rm FB}$ with $\theta_c = \pm 0.137\pi$ and $\theta_c = -0.164\pi$ which is shown in Fig. 3. Therefore the θ_c can be determined by measuring $A_{\rm FB}$ in the $\theta_c > 0$ region, and in the $\theta_c < 0$ region the θ_c can also be determined by considering both $A_{\rm FB}$ and the branching ratio in the experiments. Though the mixing angle can not be determined by only one observable like $A_{\rm FB}$ in the $\theta_c < 0$ region, the measurement of $A_{\rm FB}$ will be strong evidence of the existence of the mixing angle. The distribution of $dA_{\rm FB}/dp_\Xi^2$ shows two zero points which are around the mass poles of Ξ and Ξ' respectively, which is a strong signal of the $\Xi_c^{0/+}$-$\Xi_c'^{0/+}$ mixing effect and can be measured by future experiments.

V. SUMMARY

The angular distribution of $\Xi_c^p \to \Xi^{(\prime)}(\Lambda\pi)\ell^+\nu$ is analyzed in this work by introducing the $\Xi_c^{0/+}$-$\Xi_c'^{0/+}$ mixing effect. Due to the $\Xi_c^{0/+}$-$\Xi_c'^{0/+}$ mixing effect, the physical state Ξ_c^p can decay into $\Lambda\pi\ell^+\nu$ by the resonance Ξ'. Therefore the four-body cascade decay process $\Xi_c^p \to \Xi^{(\prime)}(\Lambda\pi)\ell^+\nu$ becomes a good platform for searching the $\Xi_c^{0/+}$-$\Xi_c'^{0/+}$ mixing effect in the experiment.

We have introduced an observable, forward-backward asymmetry $A_{\rm FB}$, which can be used to search for mixing effect and measuring the mixing angle θ_c. Compared with the differential decay width, the advantage of $A_{\rm FB}$ is that it can reflect both the Ξ and Ξ' contributions, and has a good monotonous dependency on the mixing angle θ_c.

In our numerical estimation, we achieved the value of decay width and branching fraction with $\theta_c = \pm 0.137\pi$ and $\theta_c = -0.164\pi$ in Table I. We find that the contribution of the Ξ' resonance is $\sim 10^{-12}\%$. We also estimate the value of integrated $A_{\rm FB}$ in Table I and study the θ_c and p_Ξ^2 dependence of $A_{\rm FB}$. We believe our research will provide useful guidance for searching for $\Xi_c^{0/+}$-$\Xi_c^{\prime 0/+}$ mixing effect in future experiments.

ACKNOWLEDGMENTS

We thank Professor Xiao-Gang He and Professor Wei Wang for useful discussions. This work is supported in part by Natural Science Foundation of China under Grants No. 12090064, 11735010, 11911530088, and 12147147, by Natural Science Foundation of Shanghai under Grant No. 15DZ2272100, and by China Postdoctoral Science Foundation under Grant No. 2022M72210.

APPENDIX: ANGULAR DISTRIBUTION FORMULA AND ITS COEFFICIENT FUNCTIONS

$$\begin{aligned}\frac{d\Gamma}{d\cos\theta d\cos\theta_\Lambda d\phi dp_\Xi^2 dq^2} &= \mathcal{P}(L_{11} + L_{12}\cos\theta_\Lambda + L_{13}\cos 2\theta_\Lambda + (L_{21} + L_{22}\cos\theta_\Lambda)\cos 2\phi \\ &+ (L_{31} + L_{32}\cos\theta_\Lambda + L_{33}\cos 2\theta_\Lambda)\cos\theta \\ &+ (L_{41} + L_{42}\cos 2\phi + L_{43}\cos\theta_\Lambda + L_{44}\cos 2\theta_\Lambda + L_{45}\cos 2\theta_\Lambda\cos 2\phi)\cos 2\theta \\ &+ (L_{51}\sin\theta_\Lambda + L_{52}\sin 2\theta_\Lambda)\sin\theta\cos\phi + (L_{61}\sin\theta_\Lambda + L_{62}\sin 2\theta_\Lambda)\sin 2\theta\cos\phi \\ &+ (L_{71}\sin\theta_\Lambda + L_{72}\sin 2\theta_\Lambda)\sin\theta\sin\phi + (L_{81}\sin\theta_\Lambda + L_{82}\sin 2\theta_\Lambda)\sin 2\theta\sin\phi \\ &+ (L_{91} + L_{92}\cos 2\theta_\Lambda)\sin 2\phi + (L_{101} + L_{102}\cos 2\theta_\Lambda)\sin 2\phi\cos 2\theta), \\ \mathcal{P} &= \frac{G_F^2|V_{cs}|^2}{2}\frac{(1-\widehat{m_\ell}^2)\sqrt{\lambda(m_{\Xi_c},\sqrt{p_\Xi^2},\sqrt{q^2})\lambda(\sqrt{p_\Xi^2},m_\Lambda,m_\pi)}}{(2\pi)^6 512 m_{\Xi_c}^3 p_\Xi^2}, \end{aligned} \tag{A1}$$

where $q^\mu = p_{\Xi_c}^\mu - p_\Xi^\mu$ and $\hat{m}_\ell = \frac{m_\ell}{\sqrt{q^2}}$. λ read as $\lambda(m_1,m_2,m_3) = (m_1+m_2)^2 - m_3^2)((m_1-m_2)^2 - m_3^2)$. The expressions of the coefficients L_{ij} in Eq. (A1) are given as

$$\begin{aligned}
L_{11} &= -\frac{q^2}{8}(\hat{m}_\ell^2-1)\Big(\hat{m}_\ell^2\Big(3|H^{\frac{3}{2}}_{\frac{1}{2},\frac{3}{2}}|^2 + 16|H^{\frac{1}{2}}_{\frac{1}{2},\frac{1}{2}}|^2 + 10|H^{\frac{3}{2}}_{\frac{1}{2},\frac{1}{2}}|^2 + 5|H^{\frac{3}{2}}_{\frac{1}{2},-\frac{1}{2}}|^2 + 8|H^{\frac{1}{2}}_{\frac{1}{2},-\frac{1}{2}}|^2\Big) \\
&\quad + \Big(9|H^{\frac{3}{2}}_{\frac{1}{2},\frac{3}{2}}|^2 + 16|H^{\frac{1}{2}}_{\frac{1}{2},\frac{1}{2}}|^2 + 10|H^{\frac{3}{2}}_{\frac{1}{2},\frac{1}{2}}|^2 + 15|H^{\frac{3}{2}}_{\frac{1}{2},-\frac{1}{2}}|^2 + 24|H^{\frac{1}{2}}_{\frac{1}{2},-\frac{1}{2}}|^2\Big)\Big) + ((s_{\Xi_c},s_\Xi)\to(-s_{\Xi_c},-s_\Xi)), \\
L_{12} &= -2q^2(\hat{m}_\ell^2-1)\Big(2(\hat{m}_\ell^2+1)\mathcal{R}_e\Big(H^{\frac{3}{2}}_{\frac{1}{2},\frac{1}{2}}H^{\frac{1}{2}*}_{\frac{1}{2},\frac{1}{2}}\Big) + (\hat{m}_\ell^2+3)\mathcal{R}_e\Big(H^{\frac{3}{2}}_{-\frac{1}{2},\frac{1}{2}}H^{\frac{1}{2}*}_{-\frac{1}{2},\frac{1}{2}}\Big)\Big) + ((s_{\Xi_c},s_\Xi)\to(-s_{\Xi_c},-s_\Xi)), \\
L_{13} &= \frac{3q^2}{8}(\hat{m}_\ell^2-1)\Big(-(\hat{m}_\ell^2+1)2|H^{\frac{3}{2}}_{\frac{1}{2},\frac{1}{2}}|^2 + (\hat{m}_\ell^2+3)\Big(|H^{\frac{3}{2}}_{\frac{1}{2},-\frac{1}{2}}|^2 - |H^{\frac{3}{2}}_{\frac{1}{2},\frac{3}{2}}|^2\Big)\Big) + ((s_{\Xi_c},s_\Xi)\to(-s_{\Xi_c},-s_\Xi)), \\
L_{21} &= \frac{\sqrt{3}q^2}{4}(\hat{m}_\ell^2-1)^2\mathcal{R}_e\Big(H^{\frac{3}{2}}_{\frac{1}{2},\frac{3}{2}}H^{\frac{3}{2}*}_{\frac{1}{2},-\frac{1}{2}}\Big) + ((s_{\Xi_c},s_\Xi)\to(-s_{\Xi_c},-s_\Xi)), \qquad L_{22} = -L_{21}, \\
L_{31} &= -\frac{q^2}{2}(\hat{m}_\ell^2-1)\Big(3|H^{\frac{3}{2}}_{\frac{1}{2},\frac{3}{2}}|^2 - 5|H^{\frac{3}{2}}_{\frac{1}{2},-\frac{1}{2}}|^2 - 8|H^{\frac{1}{2}}_{\frac{1}{2},-\frac{1}{2}}|^2\Big) - ((s_{\Xi_c},s_\Xi)\to(-s_{\Xi_c},-s_\Xi)), \\
L_{32} &= 8q^2(\hat{m}_\ell^2-1)\Big(\mathcal{R}_e\Big(H^{\frac{3}{2}}_{-\frac{1}{2},\frac{1}{2}}H^{\frac{1}{2}*}_{-\frac{1}{2},\frac{1}{2}}\Big)\Big) - ((s_{\Xi_c},s_\Xi)\to(-s_{\Xi_c},-s_\Xi)), \\
L_{33} &= \frac{3q^2}{2}(\hat{m}_\ell^2-1)\Big(|H^{\frac{3}{2}}_{\frac{1}{2},\frac{3}{2}}|^2 + |H^{\frac{3}{2}}_{\frac{1}{2},-\frac{1}{2}}|^2\Big) - ((s_{\Xi_c},s_\Xi)\to(-s_{\Xi_c},-s_\Xi)),
\end{aligned}$$

$$L_{41} = \frac{q^2}{8}(\hat{m}_\ell^2 - 1)^2\left(3|H^{\frac{3}{2}}_{\frac{1}{2},\frac{3}{2}}|^2 - 10|H^{\frac{3}{2}}_{\frac{1}{2},\frac{1}{2}}|^2 - 16|H^{\frac{1}{2}}_{\frac{1}{2},\frac{1}{2}}|^2 + 5|H^{\frac{3}{2}}_{\frac{1}{2},-\frac{1}{2}}|^2 + 8|H^{\frac{1}{2}}_{\frac{1}{2},-\frac{1}{2}}|^2\right) + ((s_{\Xi_c}, s_\Xi) \to (-s_{\Xi_c}, -s_\Xi)),$$

$$L_{42} = \frac{q^2}{4}(\hat{m}_\ell^2 - 1)^2\left(\sqrt{3}\mathcal{R}_e\left(H^{\frac{3}{2}}_{\frac{1}{2},\frac{3}{2}}H^{\frac{3}{2}*}_{\frac{1}{2},\frac{1}{2}}\right)\right) + ((s_{\Xi_c}, s_\Xi) \to (-s_{\Xi_c}, -s_\Xi)),$$

$$L_{43} = -2q^2(\hat{m}_\ell^2 - 1)^2\left(2\mathcal{R}_e\left(H^{\frac{3}{2}}_{\frac{1}{2},\frac{1}{2}}H^{\frac{1}{2}*}_{\frac{1}{2},\frac{1}{2}}\right) - \mathcal{R}_e\left(H^{\frac{3}{2}}_{\frac{1}{2},-\frac{1}{2}}H^{\frac{1}{2}*}_{\frac{1}{2},-\frac{1}{2}}\right)\right) + ((s_{\Xi_c}, s_\Xi) \to (-s_{\Xi_c}, -s_\Xi)),$$

$$L_{44} = -\frac{3q^2}{8}(\hat{m}_\ell^2 - 1)^2\left(|H^{\frac{3}{2}}_{\frac{1}{2},\frac{3}{2}}|^2 + 2|H^{\frac{3}{2}}_{\frac{1}{2},\frac{1}{2}}|^2 - |H^{\frac{3}{2}}_{\frac{1}{2},-\frac{1}{2}}|^2\right) + ((s_{\Xi_c}, s_\Xi) \to (-s_{\Xi_c}, -s_\Xi)),$$

$$L_{45} = -\frac{q^2}{4}(\hat{m}_\ell^2 - 1)^2\left(\sqrt{3}\mathcal{R}_e\left(H^{\frac{3}{2}}_{\frac{1}{2},\frac{3}{2}}H^{\frac{3}{2}*}_{\frac{1}{2},-\frac{1}{2}}\right)\right) + ((s_{\Xi_c}, s_\Xi) \to (-s_{\Xi_c}, -s_\Xi)),$$

$$L_{51} = -q^2 2\sqrt{2}(\hat{m}_\ell^2 - 1)\left(\sqrt{3}\mathcal{R}_e\left(H^{\frac{3}{2}}_{\frac{1}{2},\frac{3}{2}}H^{\frac{1}{2}*}_{\frac{1}{2},\frac{1}{2}}\right) - \mathcal{R}_e\left(H^{\frac{3}{2}}_{\frac{1}{2},-\frac{1}{2}}H^{\frac{1}{2}*}_{\frac{1}{2},\frac{1}{2}}\right) + \mathcal{R}_e\left(H^{\frac{3}{2}}_{\frac{1}{2},\frac{1}{2}}H^{\frac{1}{2}*}_{\frac{1}{2},-\frac{1}{2}}\right)\right) - ((s_{\Xi_c}, s_\Xi) \to (-s_{\Xi_c}, -s_\Xi)),$$

$$L_{52} = -q^2\sqrt{6}(\hat{m}_\ell^2 - 1)^2\mathcal{R}_e\left(H^{\frac{3}{2}}_{\frac{1}{2},\frac{3}{2}}H^{\frac{1}{2}*}_{\frac{1}{2},\frac{1}{2}}\right) - ((s_{\Xi_c}, s_\Xi) \to (-s_{\Xi_c}, -s_\Xi)),$$

$$L_{61} = q^2\sqrt{2}(\hat{m}_\ell^2 - 1)^2\left(-\sqrt{3}\mathcal{R}_e\left(H^{\frac{3}{2}}_{\frac{1}{2},\frac{3}{2}}H^{\frac{1}{2}*}_{\frac{1}{2},\frac{1}{2}}\right) - \mathcal{R}_e\left(H^{\frac{3}{2}}_{\frac{1}{2},-\frac{1}{2}}H^{\frac{1}{2}*}_{\frac{1}{2},\frac{1}{2}}\right) + \mathcal{R}_e\left(H^{\frac{3}{2}}_{\frac{1}{2},\frac{1}{2}}H^{\frac{1}{2}*}_{\frac{1}{2},-\frac{1}{2}}\right)\right) - ((s_{\Xi_c}, s_\Xi) \to (-s_{\Xi_c}, -s_\Xi)),$$

$$L_{62} = q^2\sqrt{\frac{3}{2}}(\hat{m}_\ell^2 - 1)^2\mathcal{R}_e\left(H^{\frac{3}{2}}_{\frac{1}{2},\frac{3}{2}}H^{\frac{1}{2}*}_{\frac{1}{2},\frac{1}{2}}\right) + ((s_{\Xi_c}, s_\Xi) \to (-s_{\Xi_c}, -s_\Xi)),$$

$$L_{71} = q^2 2\sqrt{2}(\hat{m}_\ell^2 - 1)^2\left(\mathcal{I}_m\left(H^{\frac{3}{2}}_{\frac{1}{2},-\frac{1}{2}}H^{\frac{1}{2}*}_{\frac{1}{2},\frac{1}{2}}\right) + \mathcal{I}_m\left(H^{\frac{3}{2}}_{\frac{1}{2},\frac{1}{2}}H^{\frac{1}{2}*}_{\frac{1}{2},-\frac{1}{2}}\right) + \sqrt{3}\mathcal{I}_m\left(H^{\frac{3}{2}}_{\frac{1}{2},\frac{3}{2}}H^{\frac{1}{2}*}_{\frac{1}{2},\frac{1}{2}}\right)\right) + ((s_{\Xi_c}, s_\Xi) \to (-s_{\Xi_c}, -s_\Xi)),$$

$$L_{72} = q^2\sqrt{6}(\hat{m}_\ell^2 - 1)^2\mathcal{I}_m\left(H^{\frac{3}{2}}_{\frac{1}{2},\frac{1}{2}}H^{\frac{3}{2}*}_{\frac{1}{2},\frac{3}{2}}\right) + ((s_{\Xi_c}, s_\Xi) \to (-s_{\Xi_c}, -s_\Xi)), L_{91} = -\frac{1}{2\sqrt{2}}L_{82}, \qquad L_{92} = -L_{91}$$

$$L_{81} = -q^2\sqrt{2}(\hat{m}_\ell^2 - 1)^2\left(\mathcal{I}_m\left(H^{\frac{3}{2}}_{\frac{1}{2},-\frac{1}{2}}H^{\frac{1}{2}*}_{\frac{1}{2},\frac{1}{2}}\right) + \mathcal{I}_m\left(H^{\frac{3}{2}}_{\frac{1}{2},\frac{1}{2}}H^{\frac{1}{2}*}_{\frac{1}{2},-\frac{1}{2}}\right) - \sqrt{3}\mathcal{I}_m\left(H^{\frac{3}{2}}_{\frac{1}{2},\frac{3}{2}}H^{\frac{1}{2}*}_{\frac{1}{2},\frac{1}{2}}\right)\right) - ((s_{\Xi_c}, s_\Xi) \to (-s_{\Xi_c}, -s_\Xi)),$$

$$L_{82} = -q2\sqrt{\frac{3}{2}}(\hat{m}_\ell^2 - 1)^2\mathcal{I}_m\left(H^{\frac{3}{2}}_{\frac{1}{2},\frac{1}{2}}H^{\frac{3}{2}*}_{\frac{1}{2},\frac{3}{2}}\right) + ((s_{\Xi_c}, s_\Xi) \to (-s_{\Xi_c}, -s_\Xi)), \qquad L_{101} = L_{92}, \qquad L_{102} = L_{91}. \tag{A2}$$

[1] G. Aad *et al.* (ATLAS Collaboration), Phys. Lett. B **716**, 1 (2012).
[2] S. Chatrchyan *et al.* (CMS Collaboration), Phys. Lett. B **716**, 30 (2012).
[3] D. Adey *et al.* (Daya Bay Collaboration), Phys. Rev. Lett. **121**, 241805 (2018).
[4] K. Abe *et al.* (T2K Collaboration), Nature (London) **580**, 339 (2020); **583**, E16(E) (2020).
[5] B. Abi *et al.* (Muon g-2 Collaboration), Phys. Rev. Lett. **126**, 141801 (2021).
[6] C. Hays (CDF Collaboration), Proc. Sci. ICHEP2022 (**2022**) 898.
[7] R. Aaij *et al.* (LHCb Collaboration), Nat. Phys. **18**, 277 (2022).
[8] G. Caria *et al.* (LHCb Collaboration), Phys. Rev. Lett. **124**, 161803 (2020).
[9] L. Paolucci (LHCb Collaboration), Nuovo Cimento Soc. Ital. Fis C **45**, 120 (2022).
[10] J. Xu (LHCb Collaboration), Nucl. Part. Phys. Proc. **318**, 56 (2022).
[11] S. X. Li *et al.* (LHCb Collaboration), Phys. Rev. D **103**, 072004 (2021).
[12] S. X. Li *et al.* (LHCb Collaboration), J. High Energy Phys. 03 (2022) 090.
[13] LHCb Collaboration, arXiv:2208.03262.
[14] M. Ablikim *et al.* (BESIII Collaboration), Phys. Rev. Lett. **128**, 142001 (2022).
[15] M. Ablikim *et al.* (BESIII Collaboration), Phys. Rev. D **106**, 112010 (2022).
[16] T. M. Aliev, S. Bilmis, and M. Savci, Phys. Rev. D **104**, 054030 (2021).
[17] Q. A. Zhang, J. Hua, F. Huang, R. Li, Y. Li, C. Lü, C. D. Lu, P. Sun, W. Sun, W. Wang, and Y. Yang, Chin. Phys. C **46**, 011002 (2022).
[18] Z. X. Zhao, arXiv:2103.09436.
[19] X. G. He, F. Huang, W. Wang, and Z. P. Xing, Phys. Lett. B **823**, 136765 (2021).
[20] Y. B. Li *et al.* (LHCb Collaboration), Phys. Rev. Lett. **127**, 121803 (2021).
[21] S. Acharya *et al.* (ALICE Collaboration), Phys. Rev. Lett. **127**, 272001 (2021).
[22] H. Zhong, F. Xu, Q. Wen, and Y. Gu, J. High Energy Phys. 02 (2023) 235.

[23] H. W. Ke and X. Q. Li, Phys. Rev. D **105**, 9 (2022).
[24] C. Q. Geng, X. N. Jin, and C. W. Liu, Phys. Lett. B **838**, 137736 (2023).
[25] C. W. Liu and C. Q. Geng, Phys. Rev. D **107**, 013006 (2023).
[26] C. Q. Geng, X. N. Jin, C. W. Liu, X. Yu, and A. W. Zhou, Phys. Lett. B **839**, 137831 (2023).
[27] Z. P. Xing, F. Huang, and W. Wang, Phys. Rev. D **106**, 114041 (2022).
[28] R. L. Workman *et al.* (Particle Data Group), Prog. Theor. Exp. Phys. **2022**, 083C01 (2022).
[29] F. Huang and Q. A. Zhang, Eur. Phys. J. C **82**, 11 (2022).
[30] K. Azizi, Y. Sarac, and H. Sundu, Eur. Phys. J. A **48**, 2 (2012).
[31] Y. K. Hsiao, L. Yang, C. C. Lih, and S. Y. Tsai, Eur. Phys. J. C **80**, 1066 (2020).
[32] C. Q. Geng, Y. K. Hsiao, C. W. Liu, and T. H. Tsai, J. High Energy Phys. 11 (2017) 147.
[33] R. M. Wang, M. Z. Yang, H. B. Li, and X. D. Cheng, Phys. Rev. D **100**, 076008 (2019).